

Y3.N21/5:6/3324

GOVT. DOC.

NACA TN 3324

NATIONAL ADVISORY COMMITTEE FOR AERONAUTICS

TECHNICAL NOTE 3324

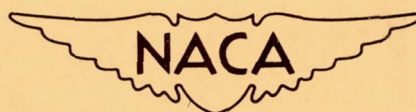
BUSINESS AND
TECHNICAL DEPT.

Jan 17 '55

A NOTE ON THE DRAG DUE TO LIFT OF RECTANGULAR
WINGS OF LOW ASPECT RATIO

By Edward C. Polhamus

Langley Aeronautical Laboratory
Langley Field, Va.



Washington

January 1955

NATIONAL ADVISORY COMMITTEE FOR AERONAUTICS

TECHNICAL NOTE 3324

A NOTE ON THE DRAG DUE TO LIFT OF RECTANGULAR

WINGS OF LOW ASPECT RATIO

By Edward C. Polhamus

SUMMARY

Methods of estimating the induced drag of low-aspect-ratio wings are discussed and compared with experiment. The profile drag due to lift is also discussed and a method is developed which relates the effect of aspect ratio on the profile drag due to lift to an "effective" two-dimensional lift coefficient. A simple expression for this effective two-dimensional lift coefficient in terms of the aspect ratio is derived and used to correlate experimental values of profile drag due to lift for rectangular wings in the low-aspect-ratio range. A method of utilizing two-dimensional test results, by means of this effective two-dimensional lift coefficient, to estimate the profile drag due to lift of low-aspect-ratio wings is briefly discussed.

INTRODUCTION

Considerable work, both experimental and theoretical, has been done with regard to the aerodynamic characteristics of low-aspect-ratio wings. Comparisons of the experimental and theoretical results have indicated that, at least for incompressible flow, the lift and pitching-moment characteristics of low-aspect-ratio wings can be estimated with reasonable accuracy. (See, for example, ref. 1.) The estimation of the drag due to lift, however, has been hampered by what appears to be a large effect of aspect ratio on the variation of profile drag with lift coefficient. The purpose of the present paper, therefore, is to attempt to determine the effect of aspect ratio on the variation of the profile drag with lift coefficient.

SYMBOLS

c_l section lift coefficient, $\frac{\text{Section lift}}{qc}$

c_l' "effective" section lift coefficient, $\frac{\text{"Effective" section lift}}{qc}$

C_L	total lift coefficient, $\frac{\text{Lift}}{qS}$
ΔC_L	portion of total lift coefficient associated with induced camber, $\frac{\text{Induced-camber lift}}{qS}$
c_d	section drag coefficient, $\frac{\text{Section drag}}{qc}$
C_D	total drag coefficient, $\frac{\text{Drag}}{qS}$
C_{D0}	drag coefficient at zero lift
ΔC_D	drag-due-to-lift coefficient, $C_D - C_{D0}$
ΔC_{Dp}	coefficient of profile drag due to lift, $\Delta C_D - C_{Di}$
C_{Di}	induced-drag coefficient, $\frac{\text{Induced drag}}{qS}$
C_N	normal-force coefficient, $\frac{\text{Normal force}}{qS}$
C_R	resultant-force coefficient, $\frac{\text{Resultant force}}{qS}$
c_s	section suction-force coefficient, $\frac{\text{Section suction force}}{qc}$
C_S	suction-force coefficient, $\frac{\text{Suction force}}{qS}$
$C_{L\alpha}$	lift-curve slope
q	dynamic pressure, $\rho V^2/2$, lb/sq ft
ρ	mass density of air, slugs/cu ft
V	free-stream velocity, ft/sec
c	wing chord, ft
S	wing area, sq ft

A	aspect ratio, b^2/S
E	Jones' edge-velocity correction factor
b	wing span, ft
α	geometric angle of attack, radians
x	longitudinal distance from wing leading edge, ft
ΔP	pressure-difference coefficient, $P_{\text{upper}} - P_{\text{lower}}$
P	local static-pressure coefficient, $\frac{p - p_o}{q}$
p_o	free-stream static pressure, lb/sq ft
p	local static pressure, lb/sq ft

ANALYSIS AND DISCUSSION

Theoretical Induced Drag

The lifting-line theory for induced drag developed by Prandtl (ref. 2) states that for an elliptical spanwise load distribution the induced drag is given by

$$C_{Di} = \frac{C_L^2}{\pi A} \quad (1)$$

The lifting-line theory, of course, neglects any effect of the vortex sheet on the chordwise loading due to induced curvature of the streamlines, and therefore it is not applicable to low-aspect-ratio wings with regard to lift and moment. Lifting-surface solutions must be used to account for this effect of the vortex sheet. With regard to the induced drag, however, Munk has pointed out (ref. 3) that the total induced drag is independent of any staggering of the lift in the stream direction and, therefore, the Prandtl lifting-line solution, with regard to induced drag, is applicable to all types of wings, provided the spanwise loading is elliptical. The theory assumes, however, that the vortex sheet lies in the plane of the wing and therefore it is strictly correct only for vanishingly small angles of attack. In an attempt to account for the effect of angle of attack, Mangler, following a proposal by A. Betz, assumes that the displacement of the vortex sheet can be treated in a manner similar to that used to predict the effect of end plates (see ref. 4).

The height of the imaginary end plates increases with angle of attack, and thus the effective aspect ratio is increased. The resulting expression for the induced drag is

$$C_{Di} = \frac{C_L^2}{\pi(A + \alpha)} \quad (2)$$

with α in radians. (It is interesting to note that an essentially equivalent result has been obtained by Weinig (ref. 5) with a momentum approach.) Inasmuch as the difference between equations (1) and (2) is appreciable only for aspect ratios of about 1.0 or less, an aspect ratio of 0.25 has been chosen for a comparison of the two theories with experimental results. This comparison is shown in figure 1 for a rectangular wing, the tests of which are described in reference 6. Inasmuch as the leading-edge radius of this wing is relatively large (approximately 0.021c), potential flow would be expected up to moderate lift coefficients and would afford a good check on the potential-flow theories. It should be pointed out that in the interest of accuracy in the low-lift range, the data presented in figure 1 were obtained from the original tabulated data and not from the plot presented in reference 6. The results indicate that the drag due to lift of this wing is considerably lower than the theoretical induced drag as given by $C_L^2/\pi A$ and is in good agreement with that given by $C_L^2/\pi(A + \alpha)$ for lift coefficients up to about 0.20. At the higher lift coefficients, apparently nonpotential flow effects cause the experimental drag due to lift to rise more rapidly than the theoretical curve for induced drag (eq. (2)). This difference in drag is considered, in the following sections, as profile drag due to lift.

Effect of Aspect Ratio on Profile Drag Due to Lift

In the preceding section, it has been shown that in the low-lift range, where the profile drag is relatively independent of lift coefficient, the drag due to lift can be predicted fairly accurately by equation (2). The problem remaining in the prediction of drag due to lift, therefore, is that of the variation of the profile drag with lift. In figure 2, the increment of profile drag due to lift ΔC_{Dp} , determined as the difference between the measured drag due to lift and the theoretical induced drag (given by eq. (2)), is presented as a function of lift coefficient for several aspect ratios. The data were obtained from reference 4 and the wings were of rectangular plan form ($A = 0.5, 1, \text{ and } 2$) with NACA 0012 root sections and NACA 0009 tip sections. The wings were tested at a Reynolds number of about 10^6 . The results indicate that the profile drag due to lift is dependent to a large extent upon the aspect ratio of the wing, with extremely high values occurring for the low-aspect-ratio wing. This, of course, indicates that the profile drag for a

three-dimensional wing at a given lift coefficient cannot be determined from corresponding two-dimensional tests at that lift coefficient. In figure 3, a similar comparison is made for wings having thinner airfoil sections (NACA 63A006) at a Reynolds number of approximately 2×10^6 . These data were obtained from semispan-model tests (unpublished) conducted at the Ames Aeronautical Laboratory of the NACA. Although the profile drag due to lift ΔC_{D_p} is considerably greater for these wings than for the thick wings of figure 2, the effect of aspect ratio is similar. The reason for the higher drag on these thin wings is that the adverse pressure gradient at the leading edge increases with decreasing leading-edge radius and thereby causes more severe separation on the thin wings. This phenomenon also accounts for the fact that the data of figure 1 are not consistent with those of either figure 2 or figure 3.

The large effect of aspect ratio on the profile drag may be associated with the fact that, as the aspect ratio decreases, the chordwise pressure gradient due to angle of attack in the vicinity of the leading edge increases as a result of the induced camber (streamline curvature) associated with the chordwise variation of the induced downwash. (See, for example, ref. 7.) This increase in the adverse pressure gradient, through its effect on separation at the leading edge, would be expected to cause an increase in the profile drag. This effect of aspect ratio on the chordwise pressure gradient is illustrated in figure 4. In the upper right-hand corner of this figure the theoretical two-dimensional chordwise pressure distribution due to angle of attack over an NACA 0012 airfoil (ref. 8) is compared with the theoretical chordwise loading at the root section of a rectangular wing of aspect ratio 0.5 that also has an NACA 0012 airfoil section.¹ The change in the chordwise pressure distribution with decreasing aspect ratio is clearly evident in figure 4 and results, as pointed out previously, in larger pressure gradients in the vicinity of the leading edge. These differences in chordwise pressure distributions are a result of the induced camber (streamline curvature) associated with the chordwise variation of induced downwash for the wing with aspect ratio of 0.5. This induced camber corresponds to a negative geometric camber and increases in magnitude with decreasing aspect ratio. In order to maintain a given lift coefficient the loss due to the induced

¹Available three-dimensional calculations are for wings of zero thickness and result in infinite pressures at the leading edge. For this comparison, however, it is more satisfactory to utilize wings that have finite pressures at the nose and, in addition, have the same airfoil section as was used for the experimental results presented in figure 2. Since from reference 9 it can be shown that the chordwise distribution of induced camber at the root of a rectangular wing is similar to the camber distribution of the NACA 65 mean line, the corresponding chordwise pressures (p. 91 of ref. 8) corrected to the proper camber load with the aid of figure 6 were combined with the angle-of-attack loading of an NACA 0012 airfoil (p. 71 of ref. 8) to obtain the results shown for $A = 0.5$.

camber, which is a maximum at the midchord and decreases to zero at the leading and trailing edges, must be compensated for by an increase in angle of attack. The angle-of-attack load, however, is a maximum at the leading edge and therefore, although the loss of lift is compensated for, the distribution along the chord is altered as illustrated in figure 4. In the lower part of this figure the chordwise pressure distribution near the nose has been "blown up" to facilitate a comparison. It can be seen that the magnitudes of the pressure near the leading edge of the wing with aspect ratio of 0.5 (solid curve) are considerably greater than those for the two-dimensional wing (long-dash curve) at the same lift coefficient, and that the lift coefficient of the two-dimensional wing would have to be approximately twice that of the wing with aspect ratio of 0.5 (long-and-short-dash curve) to develop the same pressures near the nose. This increase in lift coefficient is equal to the negative lift associated with the induced camber. It would therefore appear that boundary-layer and separation characteristics of the wing with aspect ratio of 0.5 may more nearly correspond to those of the two-dimensional airfoil operating at twice the lift coefficient. This may account for the large effect of aspect ratio on the variation of profile drag with lift coefficient shown in figures 2 and 3.

Before attempting to correlate the effect of aspect ratio on the profile-drag variation with lift on the basis of the above concept, it is interesting to note that this concept accounts for the fact, mentioned previously, that lifting-line and lifting-surface theories result in the same induced drag despite the fact that lifting-surface solutions result in a more rearward inclination of the normal force (lower Cl_α). In order to make up for this increased rearward inclination, the suction force at the nose is required to be greater by lifting-surface concepts than by lifting-line concepts. The values of the suction-force parameter C_S/C_L^2 required to incline the resultant force at the correct angle relative to the free stream were determined from the lifting-line and lifting-surface theories (see appendix) and are compared in figure 5. It will be noted that at low aspect ratios considerably greater suction is required than is given by lifting-line or two-dimensional theory but that when the suction is calculated by a two-dimensional theory (eq. (A9)) that incorporates a lift coefficient increased by ΔC_L , which corresponds to the loss due to induced camber, good agreement is obtained. The reader is referred to the appendix for a more detailed discussion of figure 5.

It now appears possible that the increment of profile drag due to lift may be independent of aspect ratio for a given value of the effective two-dimensional lift coefficient

$$c_l' = C_L \left(1 + \frac{\Delta C_L}{C_L} \right)$$

where ΔC_L is equal to the amount of induced-camber load. In the appendix, several methods of determining the induced-camber load are discussed and it is shown that to a very good approximation (for unswept wings)

$$1 + \frac{\Delta C_L}{C_L} = \sqrt{1 + \frac{4}{A^2}}$$

A plot of $1 + \frac{\Delta C_L}{C_L}$ is presented in figure 6 and it will be noted that at low aspect ratios the induced-camber load becomes rather large in comparison with the total load.

Figures 7 and 8 have been prepared in order to evaluate the degree to which the use of this effective two-dimensional lift coefficient will eliminate the effect of aspect ratio on the profile drag due to lift. In figure 7, the data of figure 2 for profile drag due to lift are replotted as a function of the effective two-dimensional lift coefficient

$$c_l' = C_L \sqrt{1 + \frac{4}{A^2}}$$

The results indicate (fig. 7) that the effect of aspect ratio shown in figure 2 can be eliminated to a large extent by use of this effective two-dimensional lift coefficient. In figure 8, the same comparison is made by use of the data for the thin wings presented in figure 3, and, although the values of ΔC_{D_p} are considerably higher than those for the thick wings (fig. 7), the effect of aspect ratio again is largely eliminated. It is probable that the degree of correlation indicated is as good as could be expected, inasmuch as effects such as those caused by possible changes in span loading with angle of attack, tip profile shape, and so forth, although relatively small in comparison with the profile drag due to lift, have not been accounted for in the determination of the induced drag.

With regard to the application of two-dimensional data in the estimation of three-dimensional drag due to lift, the preceding results indicate that two-dimensional results for a lift coefficient that is higher

(by the factor $\sqrt{1 + \frac{4}{A^2}}$) than the lift coefficient of the three-dimensional wing in question must be used.

CONCLUDING REMARKS

An important problem in connection with the prediction of the drag due to lift of low-aspect-ratio wings involves the determination of the effect of aspect ratio on the variation of profile drag with lift coefficient. In this connection the possibility of correlating the values of profile drag due to lift for wings of various aspect ratios by the use of an "effective" two-dimensional lift coefficient has been shown both theoretically and experimentally. It is shown that, to a good approximation, this effective two-dimensional lift coefficient can be

expressed as $c_l' = C_L \sqrt{1 + \frac{4}{A^2}}$ where C_L is the total lift coefficient and A is the aspect ratio. When the profile drag for several aspect

ratios was plotted as a function of $C_L \sqrt{1 + \frac{4}{A^2}}$, the effect of aspect ratio was eliminated to a large extent. This, of course, implies that when utilizing two-dimensional data to determine the three-dimensional profile drag, the two-dimensional profile drag corresponding to a higher lift coefficient must be used. Other implications are that effects that occur in two-dimensional flow (such as Reynolds number, profile shape, and so forth) will occur at progressively lower lift coefficients and be more severe as the aspect ratio is reduced.

Langley Aeronautical Laboratory,
National Advisory Committee for Aeronautics,
Langley Field, Va., September 28, 1954.

APPENDIX

DERIVATION OF AN "EFFECTIVE" TWO-DIMENSIONAL
LIFT COEFFICIENT

As pointed out in the body of the present paper, lifting-line and lifting-surface solutions result in the same expression for the induced drag $C_L^2/\pi A$ although the lift-curve slope given by lifting-surface theory is considerably lower, especially at low aspect ratios. This means that, despite the fact that the inclination of the normal force relative to the free stream given by lifting-surface theory is greater than that given by lifting-line theory, the inclination of the resultant force is the same by both theories. In order to produce the same inclination, the suction force at the leading edge, which rotates the resultant ahead of the normal, must be greater than that given by lifting-line theory. This is illustrated in figure 4 where the leading-edge suction parameter C_S/C_L^2 as determined by the various theories is compared. For a two-dimensional wing, since the suction force must, when combined with the normal force, produce a resultant lift force normal to the free stream:

$$c_s = c_l(\alpha) = \frac{c_l^2}{2\pi} \quad (A1)$$

Therefore

$$\frac{c_s}{c_l^2} = \frac{1}{2\pi} \quad (A2)$$

For a three-dimensional wing the suction must be such as to incline the resultant force rearward by the angle $C_L/\pi A$. Therefore

$$C_S = C_L \left(\alpha - \frac{C_L}{\pi A} \right) \quad (A3)$$

By lifting-line theory,

$$\alpha = \frac{C_L(A + 2)}{2\pi A}$$

Substituting the above equation into equation (A3) yields

$$C_S = C_L \left[\frac{C_L(A + 2)}{2\pi A} - \frac{C_L}{\pi A} \right]$$

which reduces to

$$\frac{C_S}{C_L^2} = \frac{1}{2\pi}$$

This equation is independent of aspect ratio and identical to the two-dimensional value which is given by equation (A2), and is shown in figure 4 as the long-and-short-dash curve. However, when the angle of attack α determined by a lifting-surface solution (ref. 10, for example) is substituted in equation (A3), it is found that the suction is greater than indicated by lifting-line theory and dependent upon the aspect ratio as shown by the solid line in figure 4. In order to extend the results to aspect ratios approaching zero, the slender-wing solution of Jones

(ref. 11), $\alpha = \frac{2C_L}{\pi A}$, may be substituted into equation (A3). This results in

$$\frac{C_S}{C_L^2} = \frac{1}{\pi A} \tag{A4}$$

and the resulting curve is presented in figure 4 as a long-dash line. Although the theory of reference 11 is for vanishingly small aspect ratios, in general it gives accurate results for the lift-curve slope up to aspect ratios of about 0.5. The dashed line in figure 5 is therefore extended up to $A = 0.5$ and it appears to be a reasonable extension of the results obtained with the aid of reference 10.

It would be interesting to see now if the increased pressures at the leading edge due to the induced camber mentioned in the body of the paper will account for the difference in suction required by lifting-line and lifting-surface theory. Now, equation (A1) gives the suction as

$$C_S = \frac{C_L^2}{\pi A}$$

This equation is correct, however, only when the induced angle is zero as in two-dimensional flow or is constant along the chord as is assumed by three-dimensional lifting-line theory. For the actual three-dimensional case, however, where the induced angle is not constant along the chord, the pressures at the nose correspond to those of a two-dimensional wing operating at a higher lift coefficient as illustrated in figure 4. This effective two-dimensional lift coefficient can be expressed as

$$c_l' = C_L \left(1 + \frac{\Delta C_L}{C_L} \right)$$

and equation (A1) for the suction can be rewritten as

$$C_S = \frac{\left[C_L \left(1 + \frac{\Delta C_L}{C_L} \right) \right]^2}{2\pi}$$

or

$$\frac{C_S}{C_L^2} = \frac{\left(1 + \frac{\Delta C_L}{C_L} \right)^2}{2\pi} \quad (A5)$$

where ΔC_L is the magnitude of the induced-camber load. The problem now reduces to the determination of the induced-camber load.

In reference 12 Jones corrected the Prandtl lifting-line equation for the lift-curve slope of elliptical wings for the effect of the reduction in velocity around the aft semiperimeter of the wing. This reduction, which is due to the fact that the semiperimeter is greater than the wing span, results in less circulation being required to satisfy the Kutta condition and thereby less lift. This "edge velocity" correction results in the following equation (for a section lift-curve slope of 2π)

$$(C_{L\alpha})_E = \frac{2\pi A}{AE + 2} \quad (A6)$$

where E is the ratio of the semiperimeter to the span of the elliptical wing and is given by the following expression

$$E = \left(\frac{\pi}{4} + \frac{1}{A} \right) \left[1 + \frac{1}{4} \left(\frac{A - \frac{4}{\pi}}{A + \frac{4}{\pi}} \right)^2 + \frac{1}{64} \left(\frac{A - \frac{4}{\pi}}{A + \frac{4}{\pi}} \right)^4 + \dots \right] \quad (A7)$$

Now it would appear that the only difference between the results obtained by equation (A6) and the exact lifting-surface solutions is the induced camber associated with the variation of downwash along the chord. Therefore

$$\frac{\Delta C_L}{C_L} = 2\pi \left[\frac{1}{C_{L\alpha}} - \frac{1}{(C_{L\alpha})_E} \right] \quad (A8)$$

where $C_{L\alpha}$ is the lifting-surface solution.

Substitution of equation (A8) into equation (A5) results in

$$\frac{C_S}{C_L^2} = \frac{\left\{ 1 + 2\pi \left[\frac{1}{C_{L\alpha}} - \frac{1}{(C_{L\alpha})_E} \right] \right\}^2}{2\pi} \quad (A9)$$

Now by utilizing the lifting-surface results for elliptical wings (ref. 10) for $C_{L\alpha}$ and equation (A6) and (A7) for $(C_{L\alpha})_E$, the suction force C_S/C_L^2 has been calculated by equation (A9) and the results compared with the exact results in figure 5. The agreement obtained appears to substantiate the assumption that the flow about the leading edge of a finite-span wing is equivalent to that about a two-dimensional wing at an effective lift coefficient that is greater than the actual finite-span lift coefficient by an amount which can be determined by use of equation (A8).

An alternate method of determining the effective two-dimensional lift coefficient $C_L \left(1 + \frac{\Delta C_L}{C_L} \right)$ which does not require that the induced camber be known is as follows. If it is assumed that the flow is non-viscous and potential, except that no suction force is developed at the leading edge, so that the resultant force is normal to the chord, the total drag for both two- and three-dimensional wings is equal to the lift times the tangent of the angle of attack:

$$\begin{aligned} c_d &= c_l \tan \alpha \\ &= \frac{c_l^2}{2\pi} \end{aligned} \quad (A10)$$

and

$$\begin{aligned} C_D &= C_L \tan \alpha \\ &= \frac{C_L^2}{C_{L\alpha}} \end{aligned} \quad (A11)$$

However, the three-dimensional drag is also equal to the corresponding two-dimensional drag plus the induced drag $C_L^2/\pi A$:

$$C_D = c_d + \frac{C_L^2}{\pi A} = \frac{c_l^2}{2\pi} + \frac{C_L^2}{\pi A} \quad (A12)$$

Therefore, from equation (A11),

$$\frac{C_L^2}{C_{L\alpha}} = \frac{c_l^2}{2\pi} + \frac{C_L^2}{\pi A} \quad (A13)$$

Solving for c_l gives

$$c_l = C_L \sqrt{\frac{2\pi}{C_{L\alpha}} - \frac{2}{A}} \quad (A14)$$

Now if the lifting-line equation for $C_{L\alpha}$,

$$C_{L\alpha} = \frac{2\pi A}{A + 2}$$

is substituted into equation (A14) it can be shown that $c_l = C_L$. However, if lifting-surface solutions are substituted for $C_{L\alpha}$ in equation (A14), it can be shown that in order for the two-dimensional drag plus the induced drag $\frac{c_l^2}{2\pi} + \frac{C_L^2}{\pi A}$ to equal the three-dimensional drag $C_L^2/C_{L\alpha}$ the section-lift coefficient must be greater than the three-dimensional lift coefficient C_L . This is the same conclusion reached previously when the induced camber was considered; a comparison of the magnitudes of the increases given by the two methods is made in the following paragraphs.

From equation (A14),

$$1 + \frac{\Delta C_L}{C_L} = \sqrt{\frac{2\pi}{C_{L\alpha}} - \frac{2}{A}} \quad (A15)$$

where ΔC_L is the increase over the three-dimensional value of C_L . From equation (A8), which was determined from a consideration of the induced camber,

$$1 + \frac{\Delta C_L}{C_L} = 1 + 2\pi \left[\frac{1}{C_{L\alpha}} - \frac{1}{(C_{L\alpha})_E} \right] \quad (A16)$$

The results of these two methods are compared in the following table where $C_{L\alpha}$ is determined from reference 10 and $(C_{L\alpha})_E$ from equations (A6) and (A7).

A	$C_{L\alpha}$	$(C_{L\alpha})_E$	$1 + \frac{\Delta C_L}{C_L}$ from -	
			eq. (A15)	eq. (A16)
6.37	4.55	4.61	1.03	1.02
2.55	2.99	3.15	1.15	1.11
1.272	1.82	2.00	1.37	1.31
.637	.99	1.13	1.79	1.79

It will be noted that fairly good agreement is obtained between the two methods and, inasmuch as equation (A15) is dependent upon results from only one theory whereas equation (A16) is dependent on the results of two theories, it is felt that equation (A15) may be somewhat more reliable and it is, of course, more convenient to use. Now if the simple but very accurate expression for $C_{L\alpha}$ developed by Helmbold (see refs. 13 and 14),

$C_{L\alpha} = \frac{2\pi A}{\sqrt{A^2 + 4}} + 2$, is substituted into equation (A15), the following is obtained:

$$1 + \frac{\Delta C_L}{C_L} = \sqrt{1 + \frac{4}{A^2}} \quad (A17)$$

Values obtained from this expression are compared in figure 6 with the results obtained from equation (A15) by using $C_{L\alpha}$ from reference 10 and good agreement is indicated.

REFERENCES

1. Flax, A. H., and Lawrence, H. R.: The Aerodynamics of Low-Aspect-Ratio Wings and Wing-Body Combinations. Rep. No. CAL-37, Cornell Aero. Lab., Inc., Sept. 1951.
2. Prandtl, L.: Theory of Lifting Surfaces. Part I. NACA TN 9, 1920.
3. Munk, Max M.: The Minimum Induced Drag of Aerofoils. NACA Rep. 121, 1921.
4. Voepel, H.: Tests on Wings of Small Aspect Ratio. Library Translation No. 276, British R.A.E., Oct. 1948.
5. Weinig, F.: Lift and Drag of Wings With Small Span. NACA TM 1151, 1947.
6. Michael, William H., Jr.: Flow Studies in the Vicinity of a Modified Flat-Plate Rectangular Wing of Aspect Ratio 0.25. NACA TN 2790, 1952.
7. Wieghardt, Karl: Chordwise Load Distribution of a Simple Rectangular Wing. NACA TM 963, 1940.
8. Abbott, Ira H., Von Doenhoff, Albert E., and Stivers, Louis S., Jr.: Summary of Airfoil Data. NACA Rep. 824, 1945. (Supersedes NACA WR L-560.)
9. Falkner, V. M. (With Appendix by Doris Lehrian): Calculated Loadings Due to Incidence of a Number of Straight and Swept-Back Wings. R. & M. No. 2596, British A.R.C., June 1948.
10. Krienes, K.: The Elliptic Wing Based on the Potential Theory. NACA TM 971, 1941.
11. Jones, Robert T.: Properties of Low-Aspect-Ratio Pointed Wings at Speeds Below and Above the Speed of Sound. NACA Rep. 835, 1946. (Supersedes NACA TN 1032.)
12. Jones, Robert T.: Correction of the Lifting-Line Theory for the Effect of the Chord. NACA TN 817, 1941.
13. Helmbold, H. B.: Der unverwundene Ellipsenflügel als tragende Fläche. Jahrb. 1942 der Deutschen Luftfahrt-forschung, R. Oldenbourg (Munich), pp. I 111 - I 113.
14. Polhamus, Edward C.: A Simple Method of Estimating the Subsonic Lift and Damping in Roll of Sweptback Wings. NACA TN 1862, 1949.

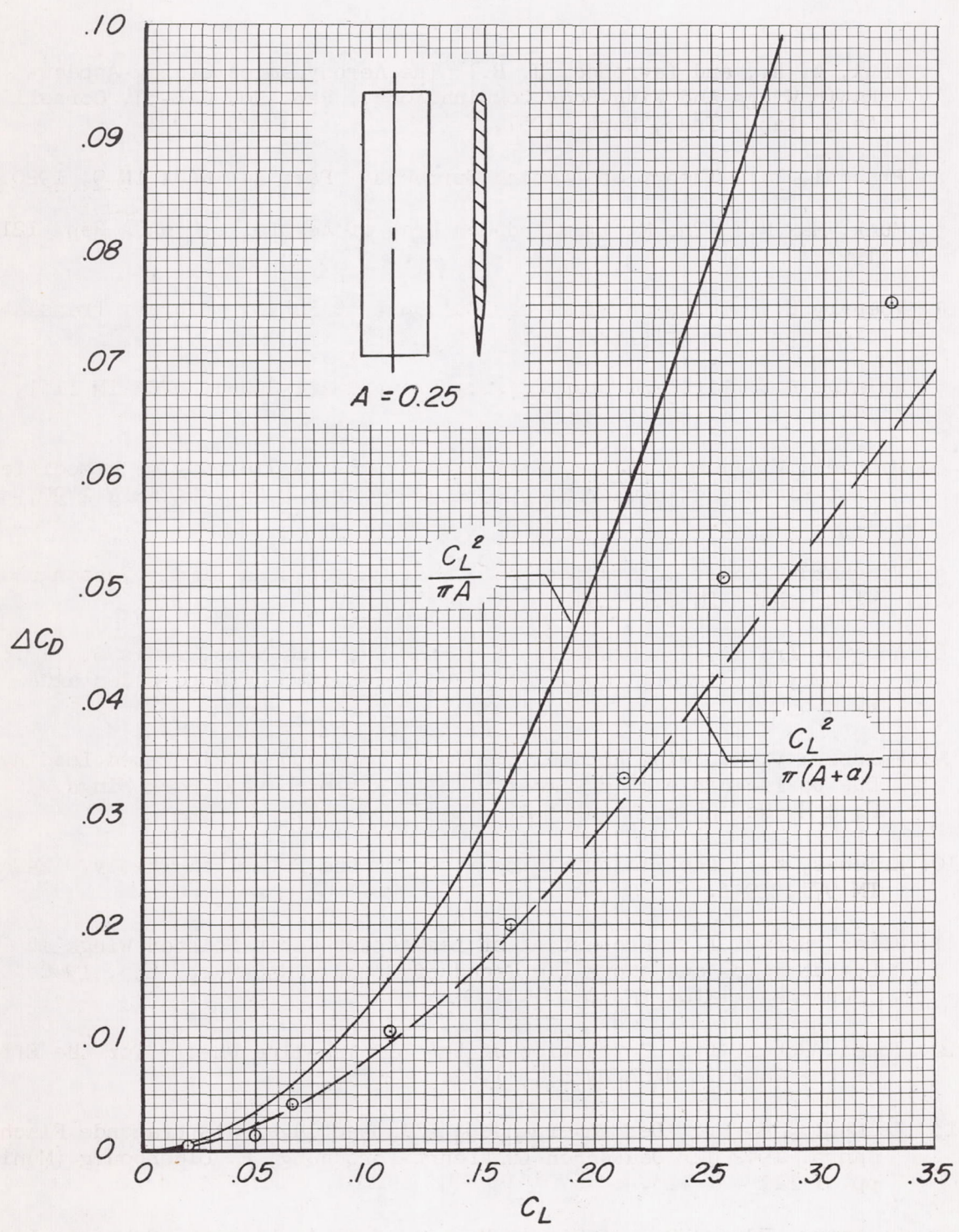


Figure 1.- Comparison of experimental drag due to lift ΔC_D with two theories for induced drag. Symbols represent experimental data from reference 6.

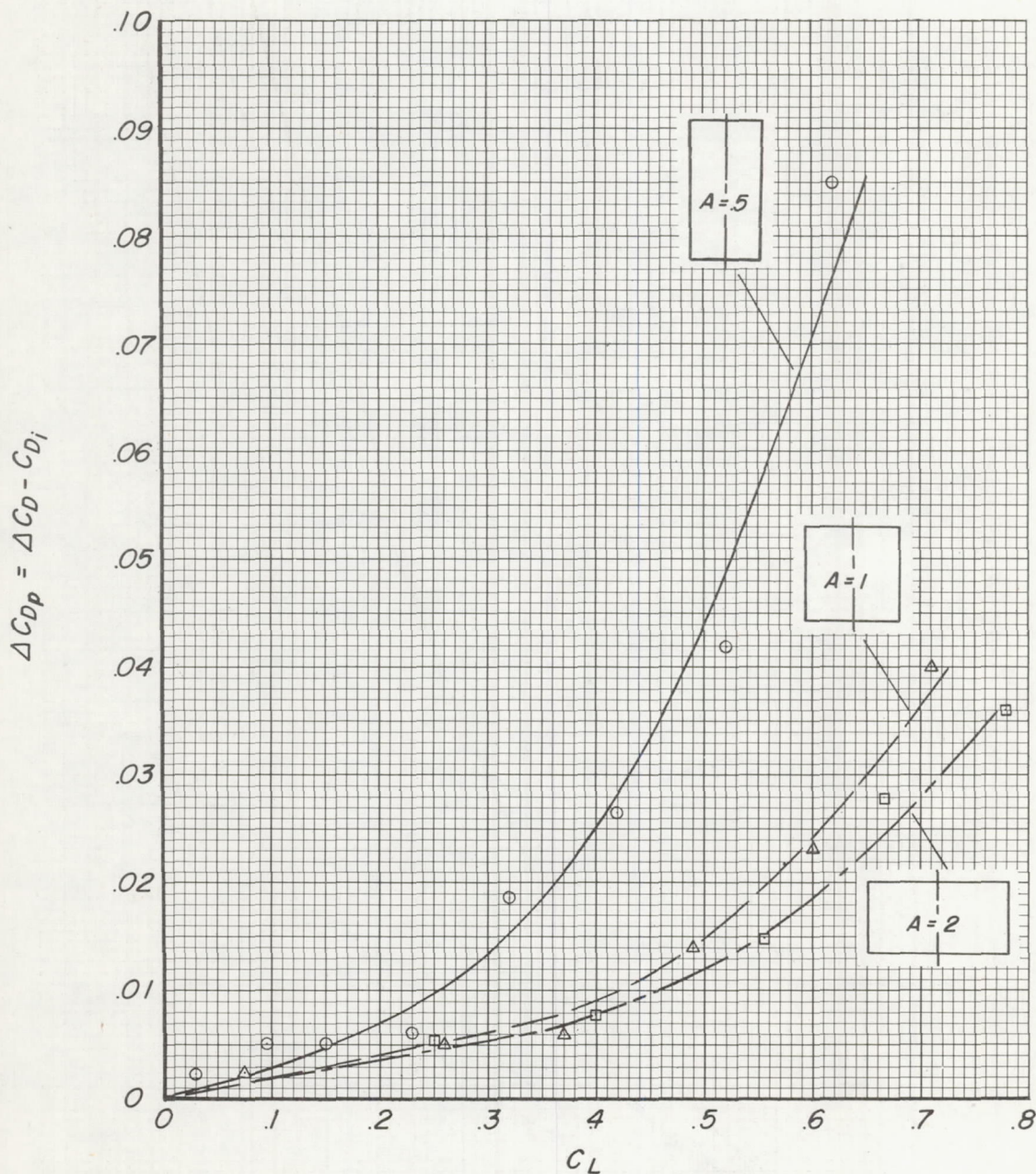


Figure 2.- Effect of wing aspect ratio on the profile drag due to lift ΔC_{Dp} .

NACA 0012 root section and NACA 0009 tip section. Data are from reference 4.

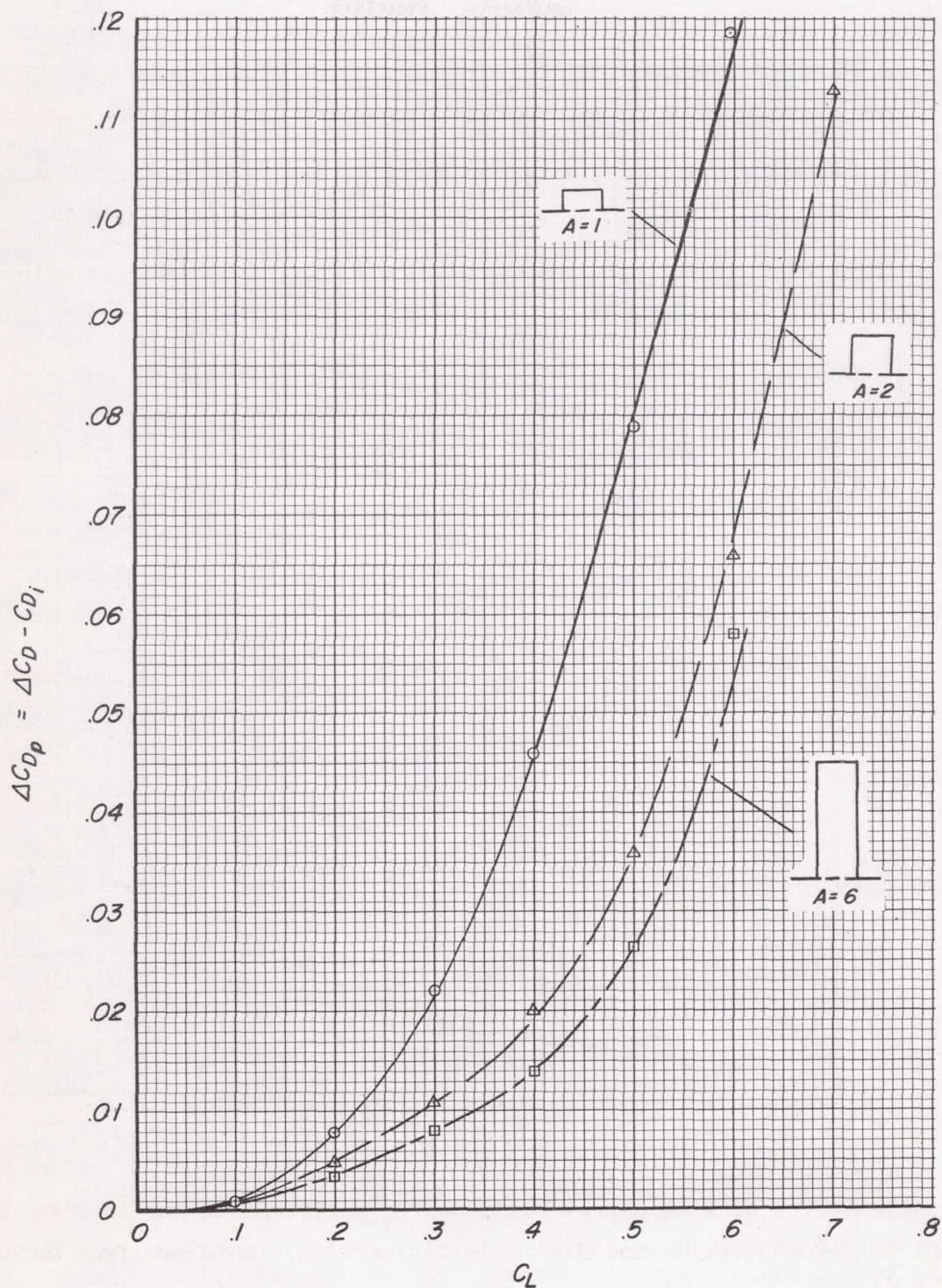


Figure 3.- Effect of wing aspect ratio on the profile drag due to lift ΔC_{Dp} .
NACA 63A006 airfoil section. Data are from tests conducted at the Ames
Aeronautical Laboratory.

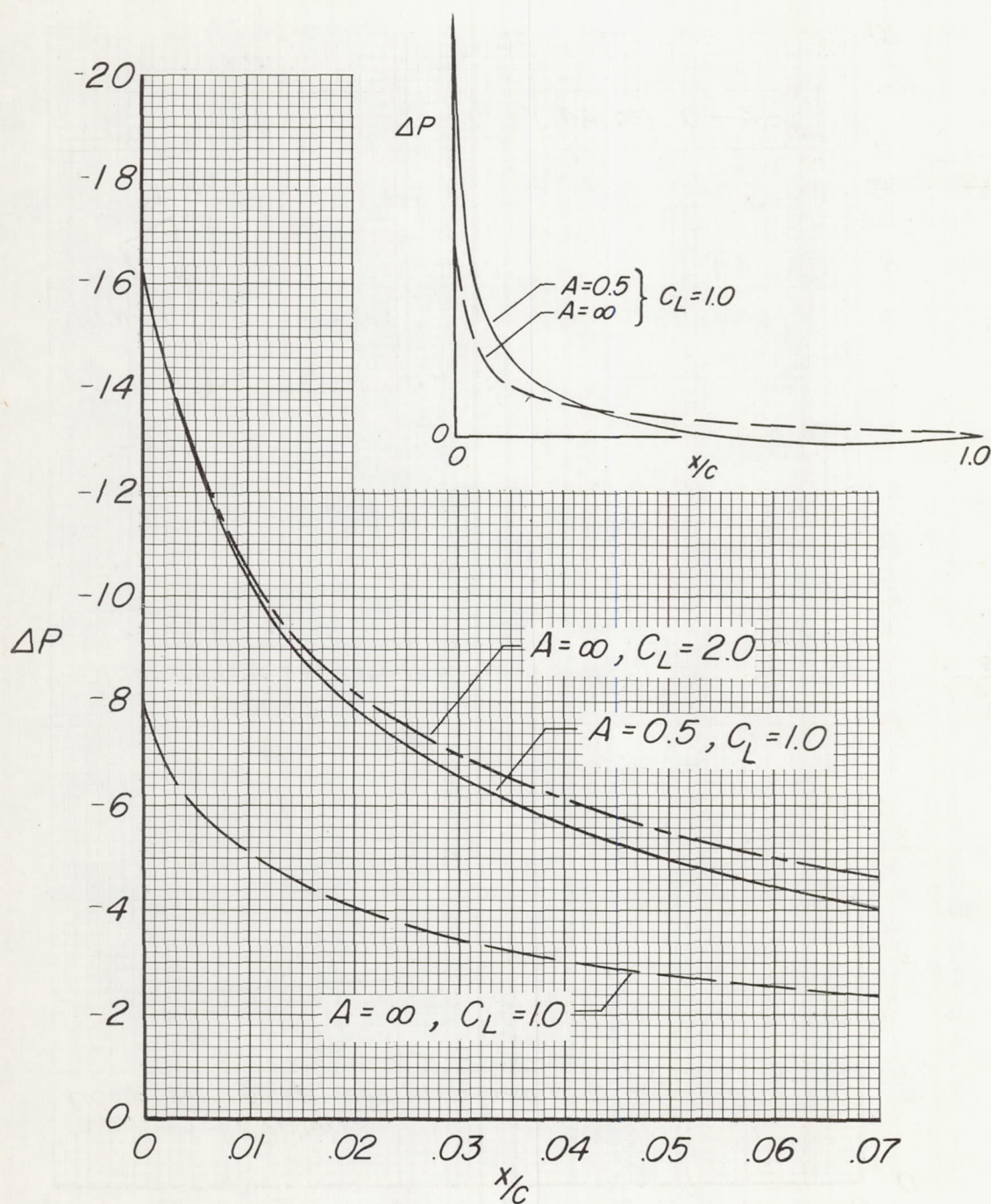


Figure 4.- Calculated effect of aspect ratio on the chordwise load distribution due to angle of attack. NACA 0012 airfoil section.

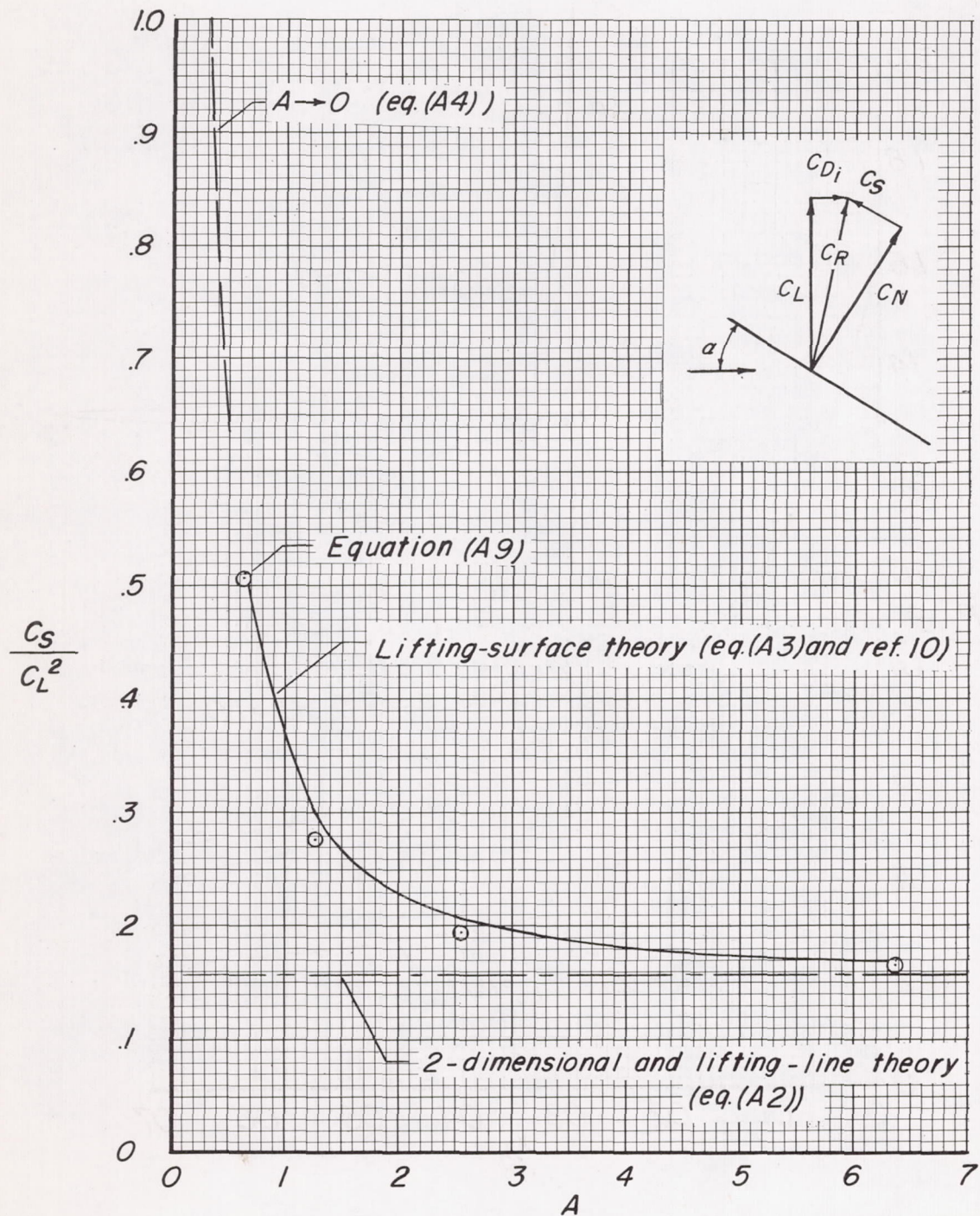


Figure 5.- Variation of leading-edge suction parameter with aspect ratio as predicted by several theories.

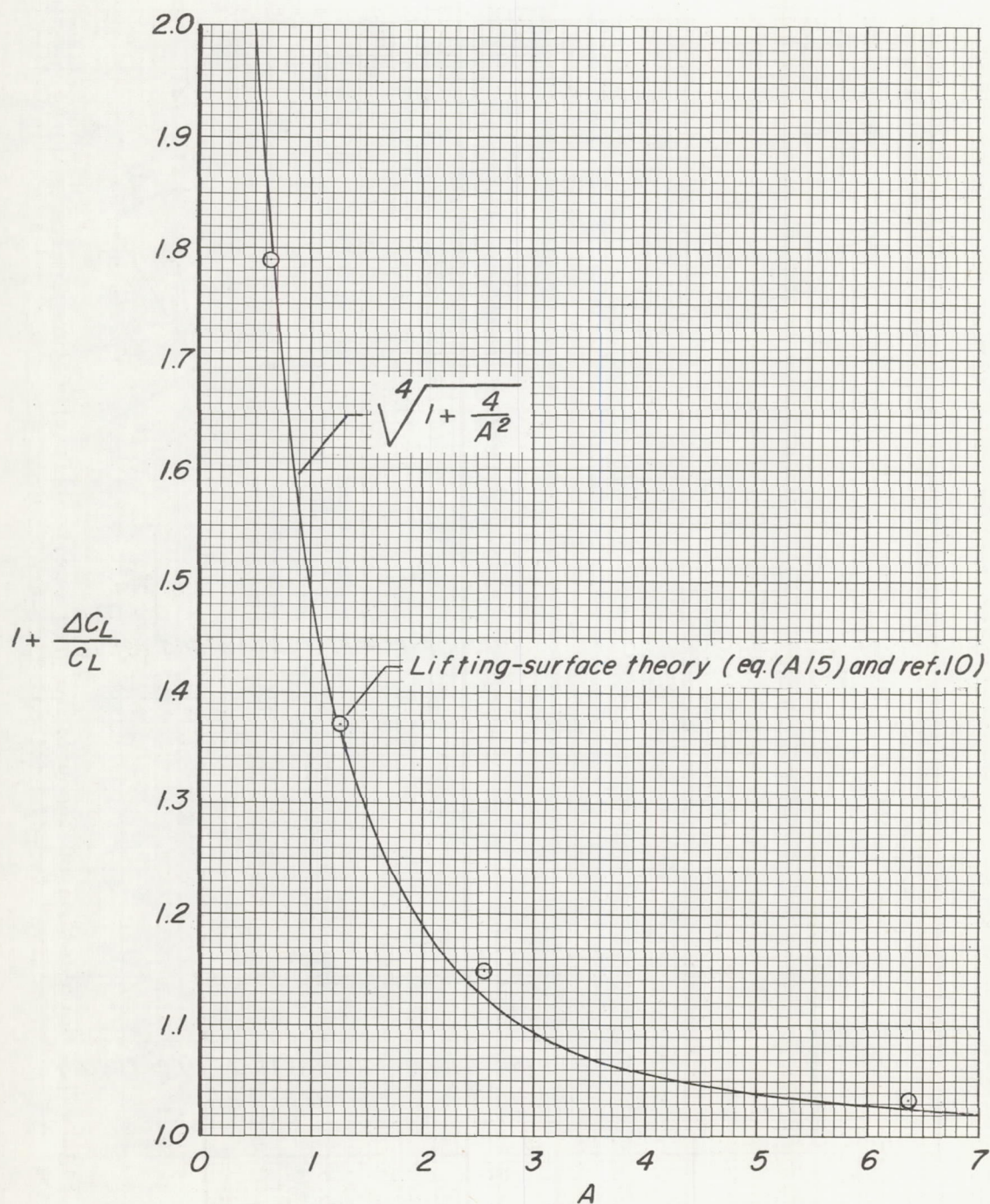


Figure 6.- Effect of aspect ratio on the induced-camber parameter $1 + \frac{\Delta C_L}{C_L}$ as predicted by two methods.

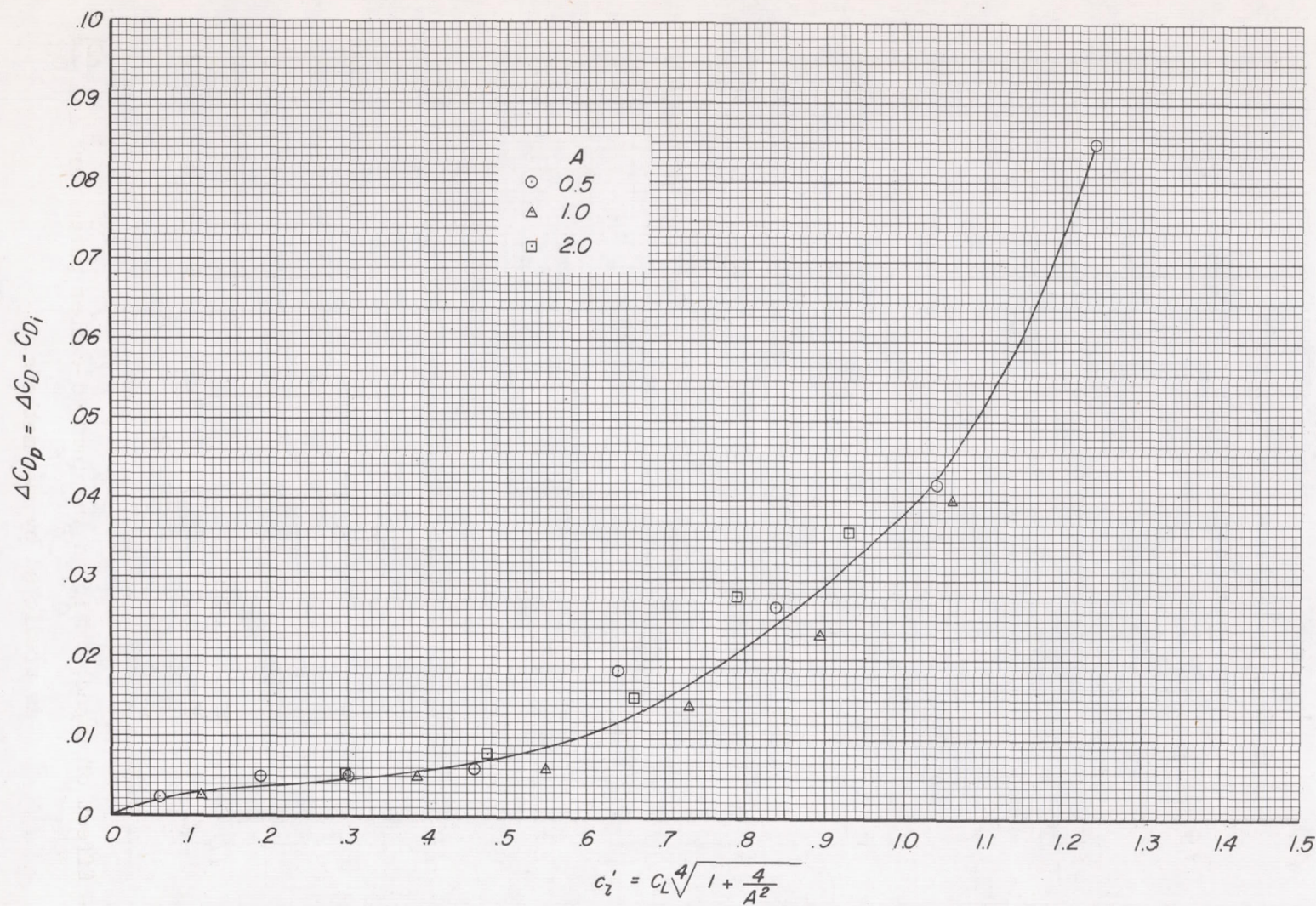


Figure 7.- Correlation of the profile drag due to lift of figure 2 with an "effective" two-dimensional lift-coefficient parameter.

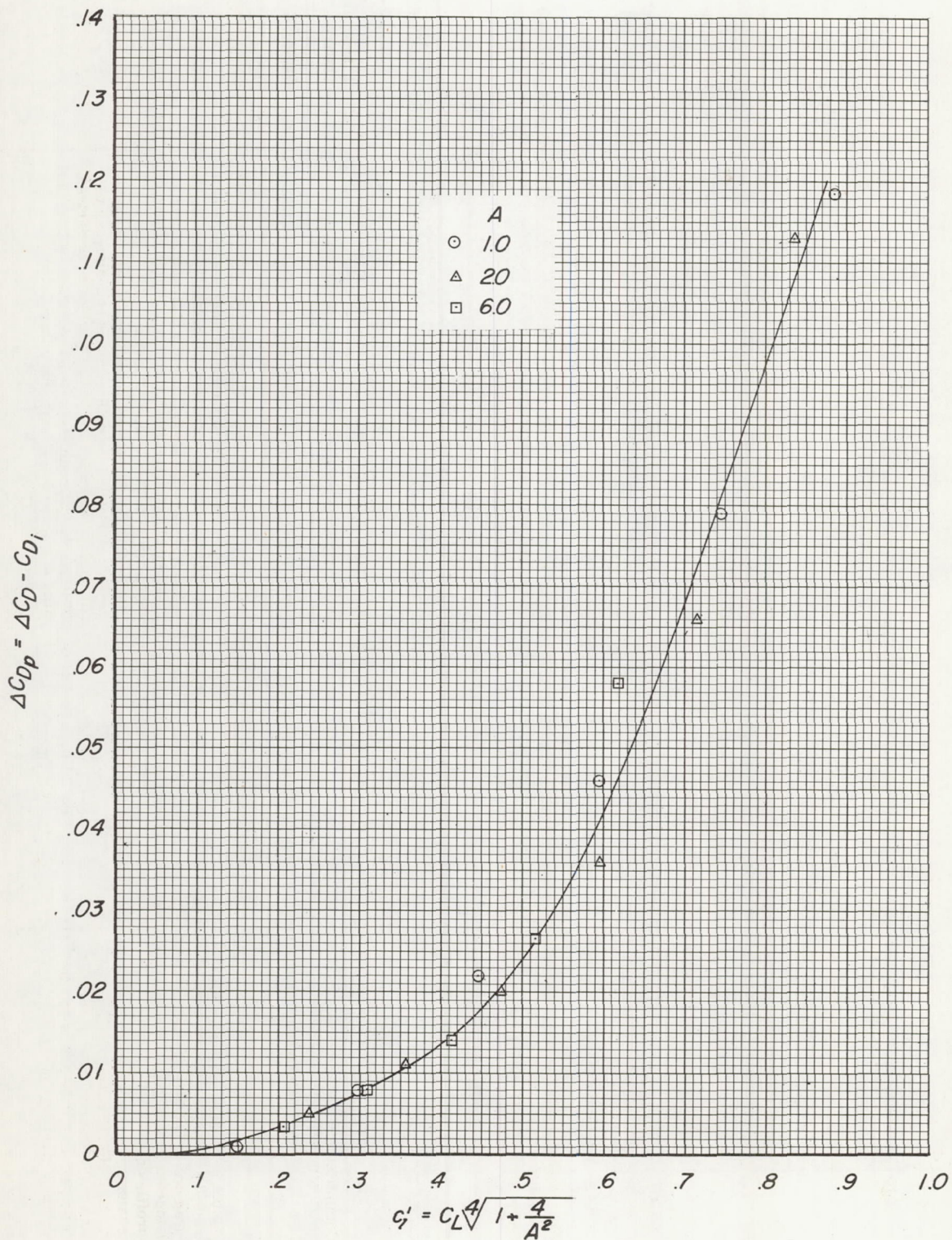


Figure 8.- Correlation of the profile drag due to lift of figure 3 with an "effective" two-dimensional lift-coefficient parameter.